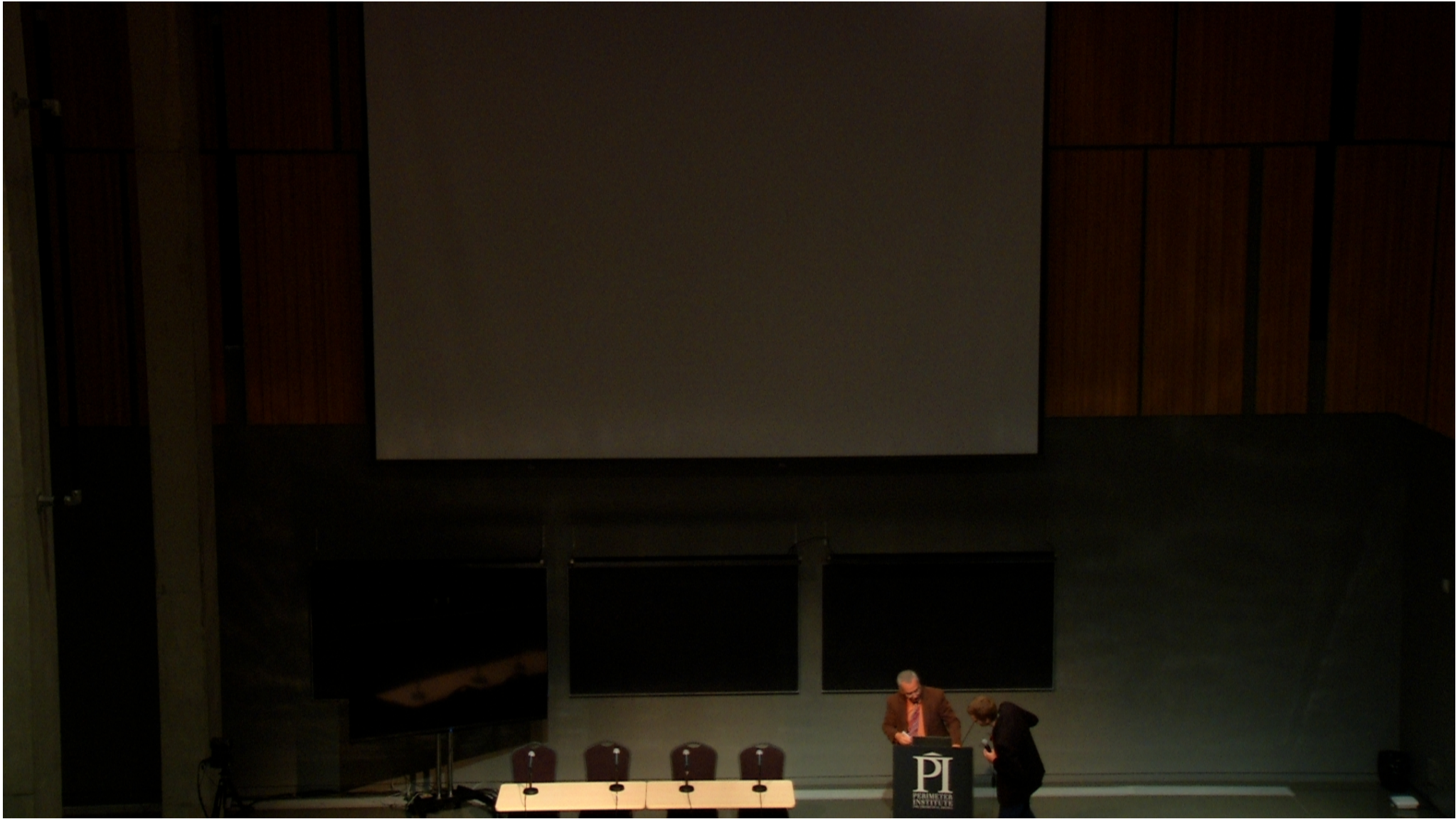


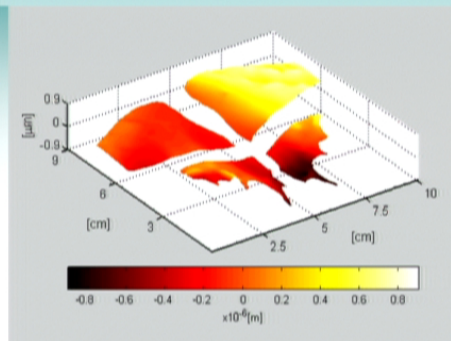
Title: 3D Digital Holographic Interferometry: Applications in Biomedicine

Date: Aug 16, 2013 04:25 PM

URL: <http://pirsa.org/13080047>

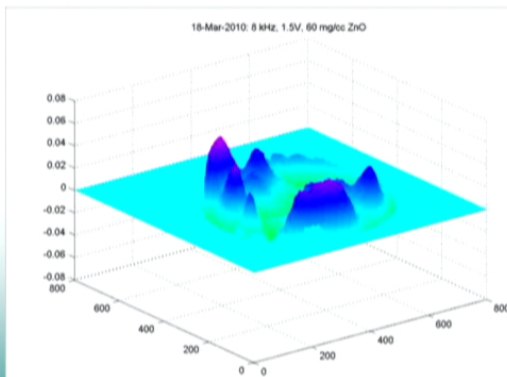
Abstract: Digital Holographic Interferometry (DHI) plays an important role in the evaluation of object static and dynamic displacements. The state of the art research on this technique is such that it is being used to solve problems in a wide variety of disciplines, from basic Physics to engineering and even social sciences. This invited plenary talk will deal with specific applications in some biomedical objects, even showing preliminary results using Electron Holography.





SCANNING VOL. 33, 342–352
(2011), and Hearing Research
263 (2010) 66–77

Optics Express, Vol. 18, No. 6
(2010), and The Virtual Journal for
Biomedical Optics Vol. 5, No. 7
(2010).



Outline of Presentation

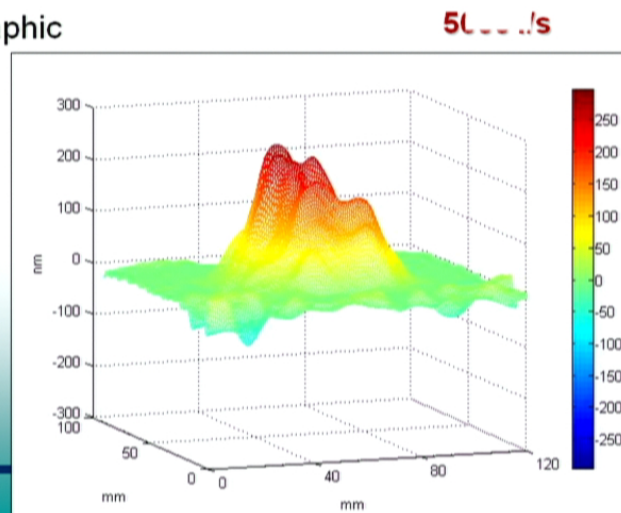
1. Introduction

- a) Interferometry: brief history and fundamentals
- b) Theory: the basics
- c) ESPI and Digital Holographic Interferometry (DHI)

2. Results:

- a) ESPI
- b) 2D y 3D DHI
- c) Bio

3. Conclusions





Definitions

Interferometry: superposition of n E-M beams in space. The result of interference depends on the phase relations between the beams.


Interference relates to the interaction between propagating beams ,
while **refraction, scattering and diffraction** depend on the interaction between a beam and matter.



A short history of interferometry

1. XVIIc. – R. Boyle, R. Hook, observation and analysis of interference effects in a thin air layer limited by two glass plates which demonstrated the wave nature of light
2. 1690 – C. Huygens, Huyghens theorem (beginning of the wave theory of light)
Each element of a wavefront may be regarded as the center of a secondary disturbance which gives rise to spherical wevelets and the position of the wevefront at any latter time is the envelope of such wevelets
3. 1738 T. Young experiment confirmed Huyghens' hipohesis and gave the basis to modern theory of light coherence
4. 1818 – A. Fresnel – extension of Huyghens theorem, leading to so-called Huyghens-Fresnel principle - great importance in the diffraction theory and the basic postulate of the wave theory of light, development of stellar interferometry

1a. 1874 Lord Rayleigh used for the first time moire phenomenon ⁵



A short history of interferometry

5. 1881 – Michelson experiment (speed of light) and his further works on interferometry, stellar interferometry, high resolution interferometric spectroscopy - he is considered as the father of interferometry (Nobel prize 1907)
6. 1916 – F. Twyman modifications of Michelson ineterferometer
7. 1960 – invention of laser: Schawlow, Maiman, Townes, Prochorow....
8. 1948 – Gabor principles of holography
9. 1962 -Leith and Upatnieks off-axis holography and development of holographic interferometry (works of Burch, Brooks, Collier, Stetson...)
10. 1970 – Archbold, Leendertz speckle interferometry and speckle photography
11. 1982- ..Development of phase based interferogram analysis methods
11. 1995-....Rapid progress in digital holography
12. 2000-...Rapid progress in active interferometry and holography

6

Fundamentals of interferometry

Vector of electric field

$$\bar{E}_i(\bar{r}, t) = \bar{E}_{i0} \exp[i(\varphi_i(\bar{r}) - \omega_i t)]$$

Resultant vector in two beam interferometry

$$\bar{E}(\bar{r}, t) = \sum_i \bar{E}_i(\bar{r}, t); \quad i = 1, 2$$

Result of two beam interference (E field intensity):

$$I(\bar{r}) \propto |\bar{E}|^2 = |\bar{E}_1 + \bar{E}_2|^2 = (\bar{E}_1 + \bar{E}_2)(\bar{E}_1 + \bar{E}_2)^* = \bar{E}_1 \bar{E}_1^* + \bar{E}_2 \bar{E}_2^* + \bar{E}_1 \bar{E}_2^* + \bar{E}_1^* \bar{E}_2$$

$$I(\bar{r}) = I_1 + I_2 + I_{12} = I_1 + I_2 + 2\sqrt{I_1 I_2} \cos[(\varphi_1(\bar{r}) - \varphi_2(\bar{r})) - (\omega_1 t - \omega_2 t)]$$

Conditions for stationary interference field:

$$\omega_1 = \omega_2$$

$$\varphi_1(\bar{r}) - \varphi_2(\bar{r}) = \text{const}$$

Recommended: parallel polarization of beams

Fundamentals of interferometry

Vector of electric field

$$\bar{E}_i(\bar{r}, t) = \bar{E}_{i0} \exp[i(\varphi_i(\bar{r}) - \omega_i t)]$$

Resultant vector in two beam interferometry

$$\bar{E}(\bar{r}, t) = \sum_i \bar{E}_i(\bar{r}, t); \quad i = 1, 2$$

Result of two beam interference (E field intensity):

$$I(\bar{r}) \propto |\bar{E}|^2 = |\bar{E}_1 + \bar{E}_2|^2 = (\bar{E}_1 + \bar{E}_2)(\bar{E}_1 + \bar{E}_2)^* = \bar{E}_1 \bar{E}_1^* + \bar{E}_2 \bar{E}_2^* + \bar{E}_1 \bar{E}_2^* + \bar{E}_1^* \bar{E}_2$$

$$I(\bar{r}) = I_1 + I_2 + I_{12} = I_1 + I_2 + 2\sqrt{I_1 I_2} \cos[(\varphi_1(\bar{r}) - \varphi_2(\bar{r})) - (\omega_1 t - \omega_2 t)]$$

Conditions for stationary interference field:

$$\omega_1 = \omega_2$$

$$\varphi_1(\bar{r}) - \varphi_2(\bar{r}) = \text{const}$$

Recommended: parallel polarization of beams

Fundamentals of interferometry

Vector of electric field

$$\bar{E}_i(\bar{r}, t) = \bar{E}_{i0} \exp[i(\varphi_i(\bar{r}) - \omega_i t)]$$

Resultant vector in two beam interferometry

$$\bar{E}(\bar{r}, t) = \sum_i \bar{E}_i(\bar{r}, t); \quad i = 1, 2$$

Result of two beam interference (E field intensity):

$$I(\bar{r}) \propto |\bar{E}|^2 = |\bar{E}_1 + \bar{E}_2|^2 = (\bar{E}_1 + \bar{E}_2)(\bar{E}_1 + \bar{E}_2)^* = \bar{E}_1 \bar{E}_1^* + \bar{E}_2 \bar{E}_2^* + \bar{E}_1 \bar{E}_2^* + \bar{E}_1^* \bar{E}_2$$

$$I(\bar{r}) = I_1 + I_2 + I_{12} = I_1 + I_2 + 2\sqrt{I_1 I_2} \cos[(\varphi_1(\bar{r}) - \varphi_2(\bar{r})) - (\omega_1 t - \omega_2 t)]$$

Conditions for stationary interference field:

$$\omega_1 = \omega_2$$

$$\varphi_1(\bar{r}) - \varphi_2(\bar{r}) = \text{const}$$

Recommended: parallel polarization of beams

Fundamentals of interferometry

For $\omega_1 = \omega_2$ (usually one source applied)

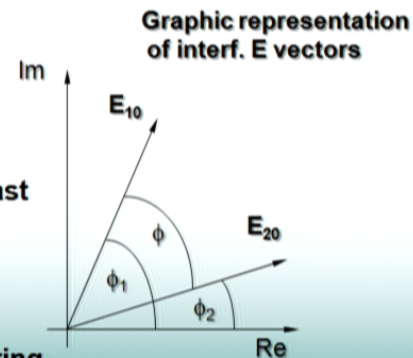
$$I(\vec{r}) = I_1 + I_2 + 2\sqrt{I_1 I_2} \cos(\varphi_1(\vec{r}) - \varphi_2(\vec{r})) = a(\vec{r}) + b(\vec{r}) \cos \varphi(\vec{r}) \cong 1 + \gamma(\vec{r}) \cos \varphi(\vec{r})$$

Where $a(r)$ and $b(r)$ are background and fringe modulation functions

$$\gamma = \frac{2\sqrt{I_1 I_2}}{I_1 + I_2} \quad \text{is the interferogram contrast}$$

$$\varphi(\vec{r}) = \varphi_1(\vec{r}) - \varphi_2(\vec{r})$$

is the phase difference between the interfering beams





The observable physical quantity is the intensity,

$$I = |a|^2 = (a_1 + a_2)(a_1^* + a_2^*) =$$
$$A_1^2 + A_2^2 + A_1A_2 e^{i(\varphi_2 - \varphi_1)} + A_1A_2 e^{-i(\varphi_2 - \varphi_1)} =$$
$$I_1 + I_2 + 2\sqrt{I_1I_2} \cos \Delta\varphi \quad (3)$$

where $\Delta\varphi = \varphi_1 - \varphi_2$.

Output: interferogram





Modifications to interferograms help retrieve the imbedded phase

$$I(x, y, t) = a(x, y) + b(x, y) \cos[2\pi [(f_{0x}x + f_{0y}y) + \nu_0(t)] + \alpha(t) + \phi(x, y)]$$

Required controlled modifications of phase in FP:

$\nu_0(t)$ – introduces temporal heterodyning (running fringes)

$\alpha(t)$ – introduces controlled phase shifts

f_{0x}, f_{0y} – introduce spatial carrier fringes (spatial heterodyning)

However the requirement to get a high quality interferogram:

Source with spatial and temporal coherence.



Modifications to interferograms help retrieve the imbedded phase

$$I(x, y, t) = a(x, y) + b(x, y) \cos[2\pi [(f_{0x}x + f_{0y}y) + \nu_0(t)] + \alpha(t) + \phi(x, y)]$$

Required controlled modifications of phase in FP:

$\nu_0(t)$ – introduces temporal heterodyning (running fringes)

$\alpha(t)$ – introduces controlled phase shifts

f_{0x}, f_{0y} – introduce spatial carrier fringes (spatial heterodyning)

However the requirement to get a high quality interferogram:

Source with spatial and temporal coherence.

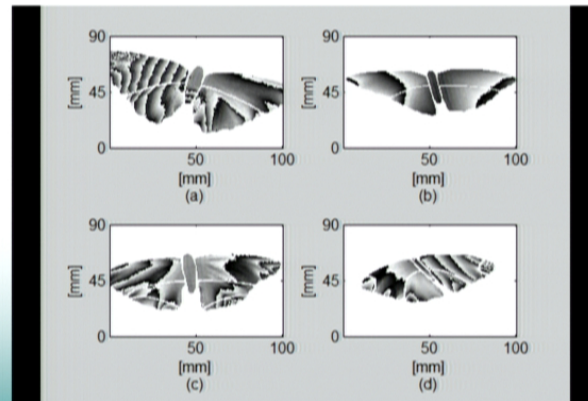
Available measurement methods

Electronical
Mechanical
Optical →
Acoustical
Pneumatics
.....

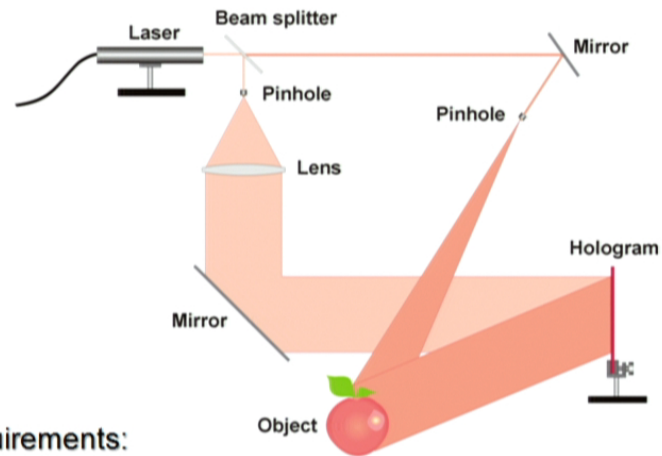
Photo elasticity
Optical fiber sensors
Moiré (fringe projection)
Speckle photography
Shearography
Laser vibrometer (high temporal,
low spatial resolution)
Digital holographic
interferometry (high spatial, low
temporal resolution)
.....

Holography and speckle techniques

Holographic and speckle interferometry



Registration of optical hologram basic setup



Requirements:

1. Need to have equal optical paths of reference and object beams (within coherence length of laser)
2. During recording the phase between object and reference beams cannot change more than

$$\Delta\phi_{\max} < 0.2\pi$$

Basic Theoretical Considerations

Two wave addition: Object and Reference

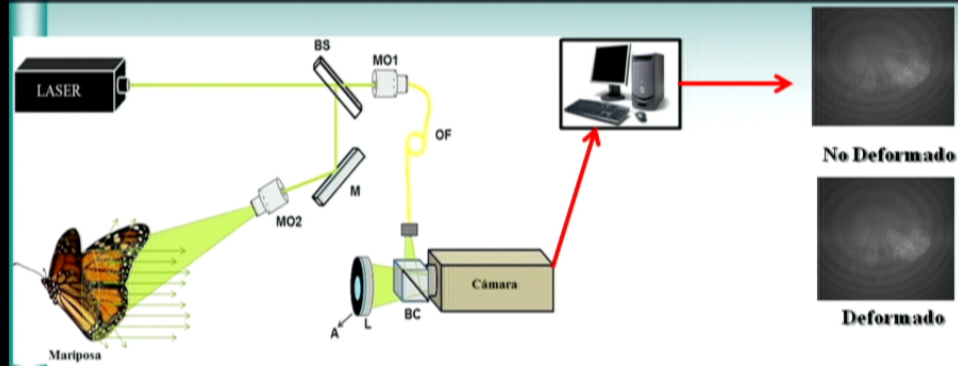
$$U_T = U_o + U_r \quad (1)$$

Intensity/Irradiance on the CCD sensor is proportional to

$$I_T = U_o^* U_o + U_r^* U_r + U_o U_r^* + U_r U_o^* \quad (2)$$



Digital Holographic Interferometry (DHI)



Limitations of digital holography


The recording medium has to fulfil the Nyquist condition !
Each fringe has to be sampled by at least two pixels of CCD matrix

CCD cameras;

- resolution 1024x1534;

- Pixel size $\Delta=9\mu\text{m}$; for $4.5\ \mu\text{m}$

- Spatial resolution - ap. 111 lines/mm, 220l/mm

holographic materials (plates) - >3000 lines/mm).  Limitations

$$\delta = \lambda / (2 \sin(\gamma/2))$$

Assumption.: $\gamma \approx \sin \gamma \approx \tan \gamma$
For small γ

$$\gamma \leq \lambda / (2\Delta)$$

$$2\Delta \leq \delta$$

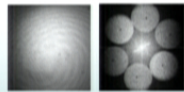
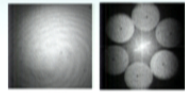
=>

for $\lambda=632.8\text{nm}$ and $\Delta=9\mu\text{m}$, $\gamma \approx 3.5^\circ$

**Conclusion: SMALL angular size of object (a few degrees)
i.e.
SMALL OBJECT or Object SITUATED FAR from CAMERA**

18

Phase evaluation with 3 holograms

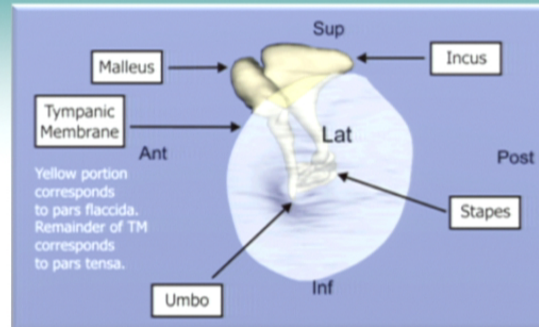




Tympanic Membrane



Endoscopic image of the TM



Characteristics of human TM

Semitransparent

Cone shaped

The depth of the cone is about 1.5 mm

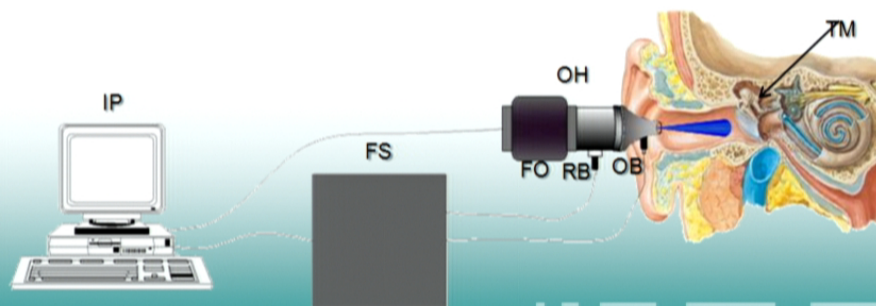
Diameter is 8-10 mm

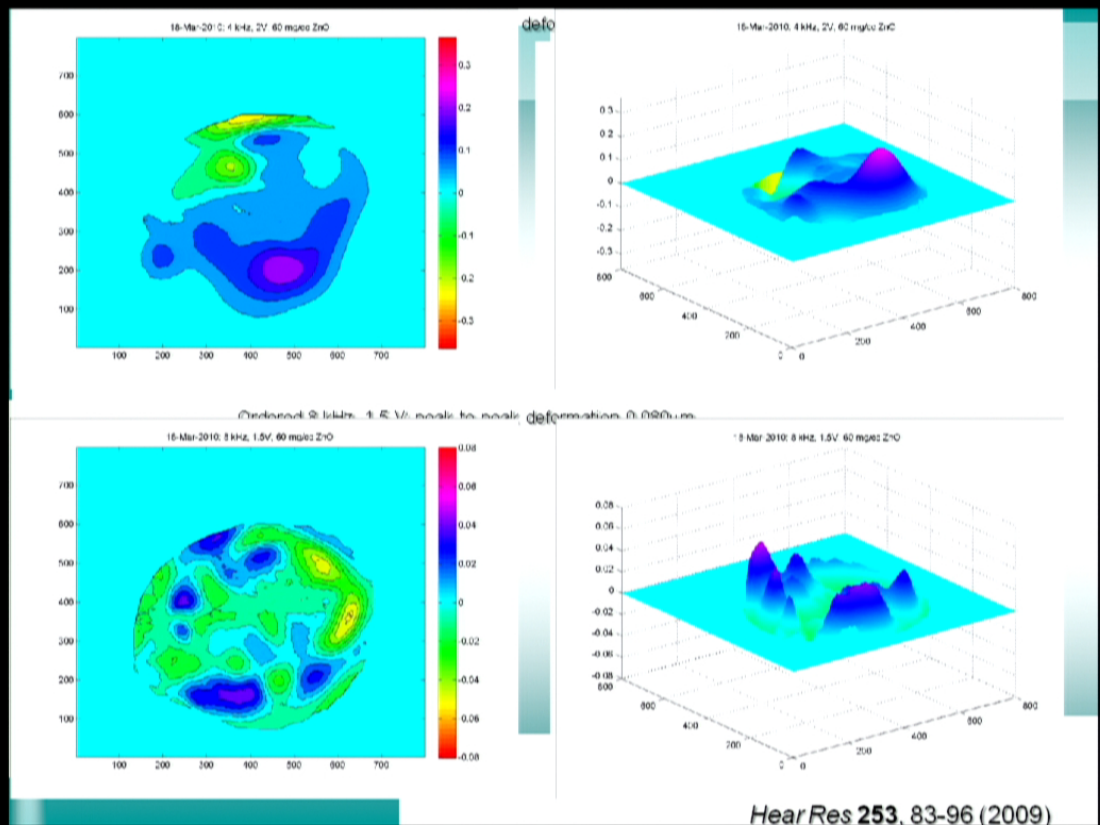
Thickness varies between 55 and 140 μm

OEHO System

The inspection system consists of:

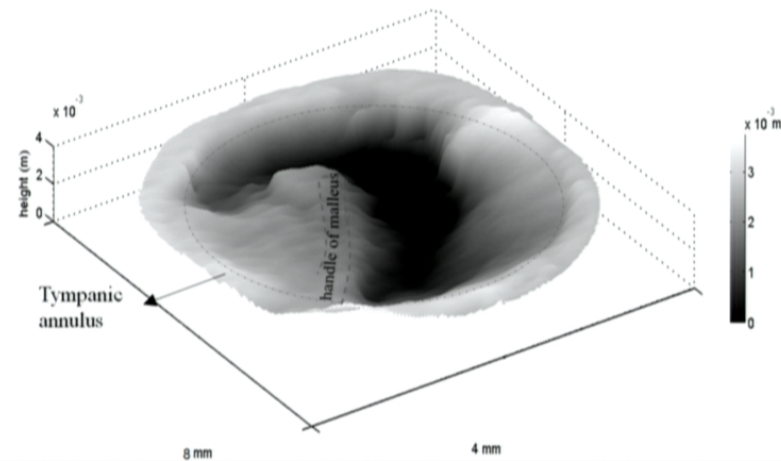
- High speed PC with dedicated software and hardware,
- Fiber optics, FS, and
- A compact optics head resembling an otoscope, OH





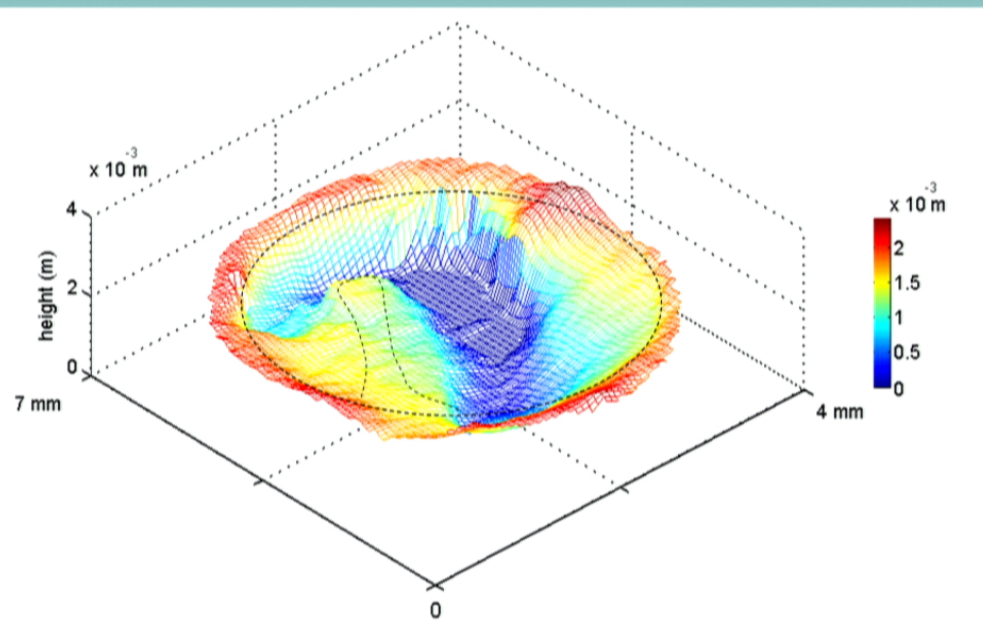
The TM surface height-change may be found from the difference between the reconstructed phases which are recorded before and after the small tilt of the object illuminating beam by the follow equation:

$$\Delta\varphi = 2K \sin \frac{\Delta\theta}{2} \left[x \cos \left(\theta + \frac{\Delta\theta}{2} \right) - h(x) \sin \theta + \frac{\Delta\theta}{2} \right]$$



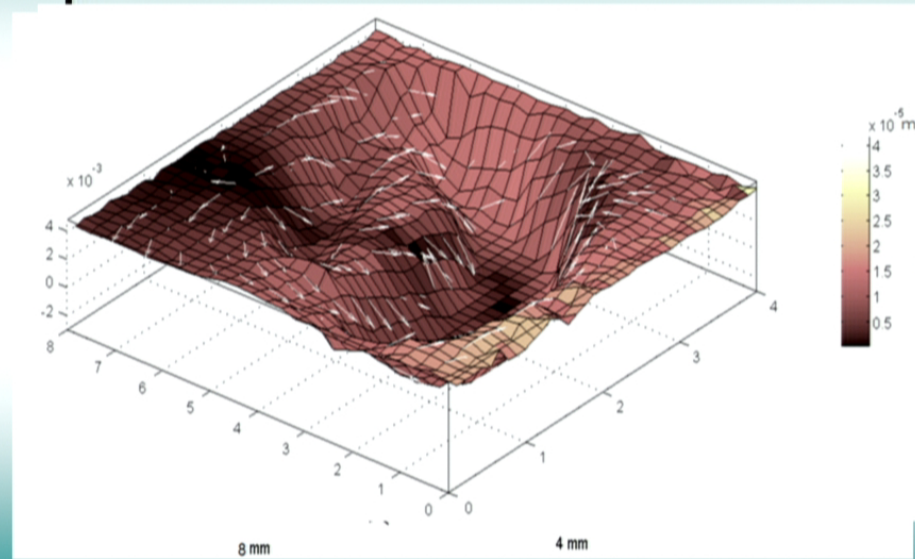


Shown : Tympanic annulus and handle of maleus





3D Displacement on the TM shape

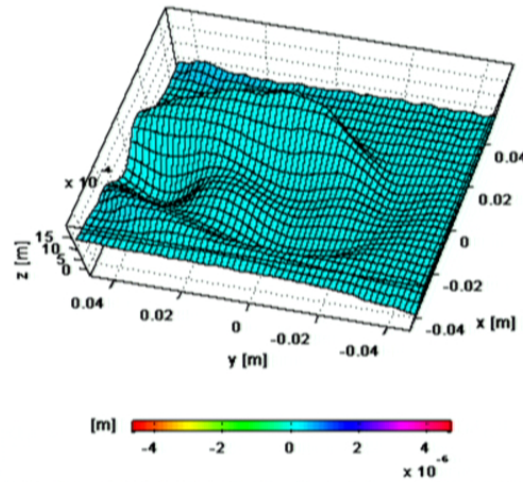




INHOMOGENEITIES DETECTION (TUMORS)

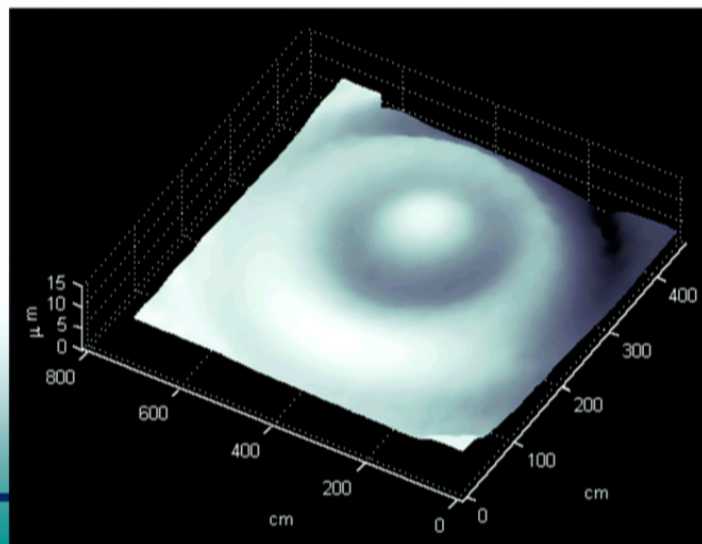
- Input sound power of approximately 661 mW, equivalent to a pressure of 2.3×10^5 pa.
- Laser pulse separation 14 ms, at 532 nm, 15 ns pulse width, 20 mJ/pulse, average power of $0.639 \mu\text{W}/\text{cm}^2$ at the surface, and 6 m of coherence length.
- CCD with 1024 by 1280 pixels at 12 bits.
- Phantom is a semi sphere with an 8.4 cm in diameter and 4 cm height.

Unwrapped phase map without sound,
gel surface free to move due to environmental
disturbances

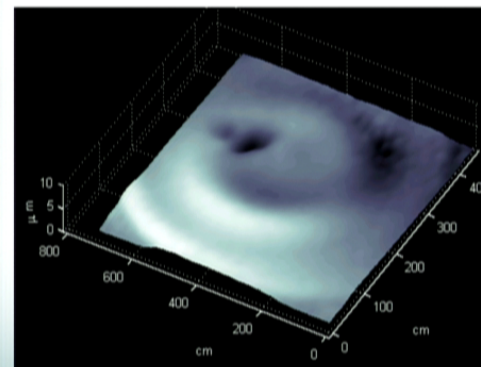
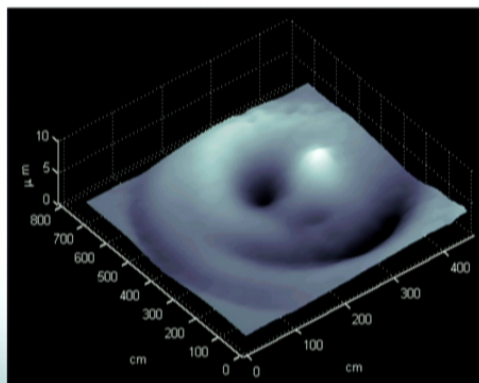


It is not possible to
observe whether
there is an
inhomogeneity in
the gel

Without inhomogeneity and sound:
resonant mode at 810 Hz.

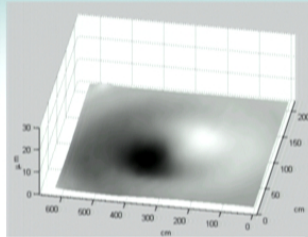


With inhomogeneity: Malignant tumor 10 mm diameter

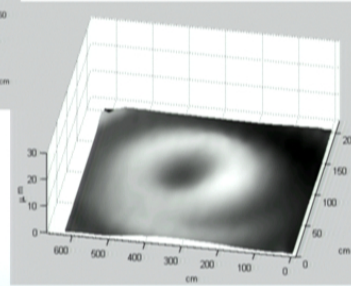


With 3D data the depth of the tumor may be found

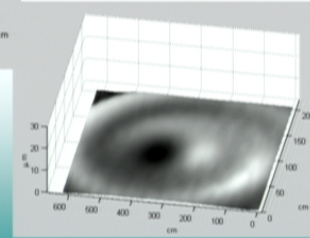
Unwrapped phase maps corresponding to each illumination direction



L



C



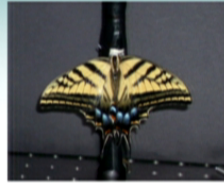
R



Butterflies in-flight



Capture



Fixing



experimental
measurement



44



Comparison among 4 butterflies



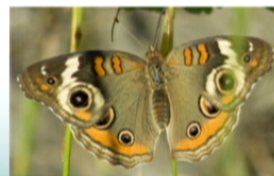
Pterourus Multicaudata



Agraulis Vanillae Incarnata



Danaus Gillipus Cramer



Precis Evarete Felder



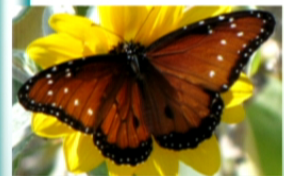
Comparison among 4 butterflies



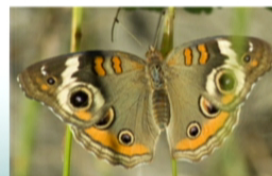
Pterourus Multicaudata



Agraulis Vanillae Incarnata



Danaus Gillipus Cramer

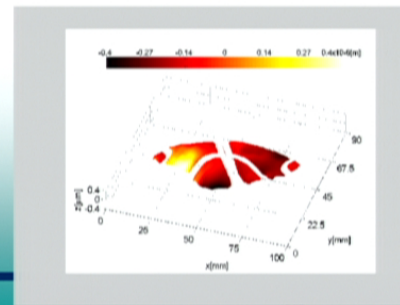
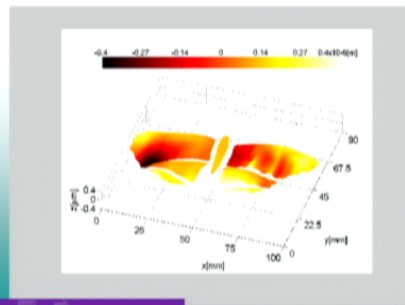
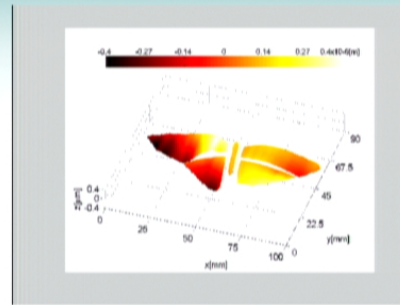
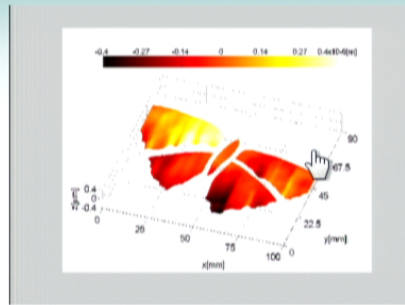


Precis Evarete Felder

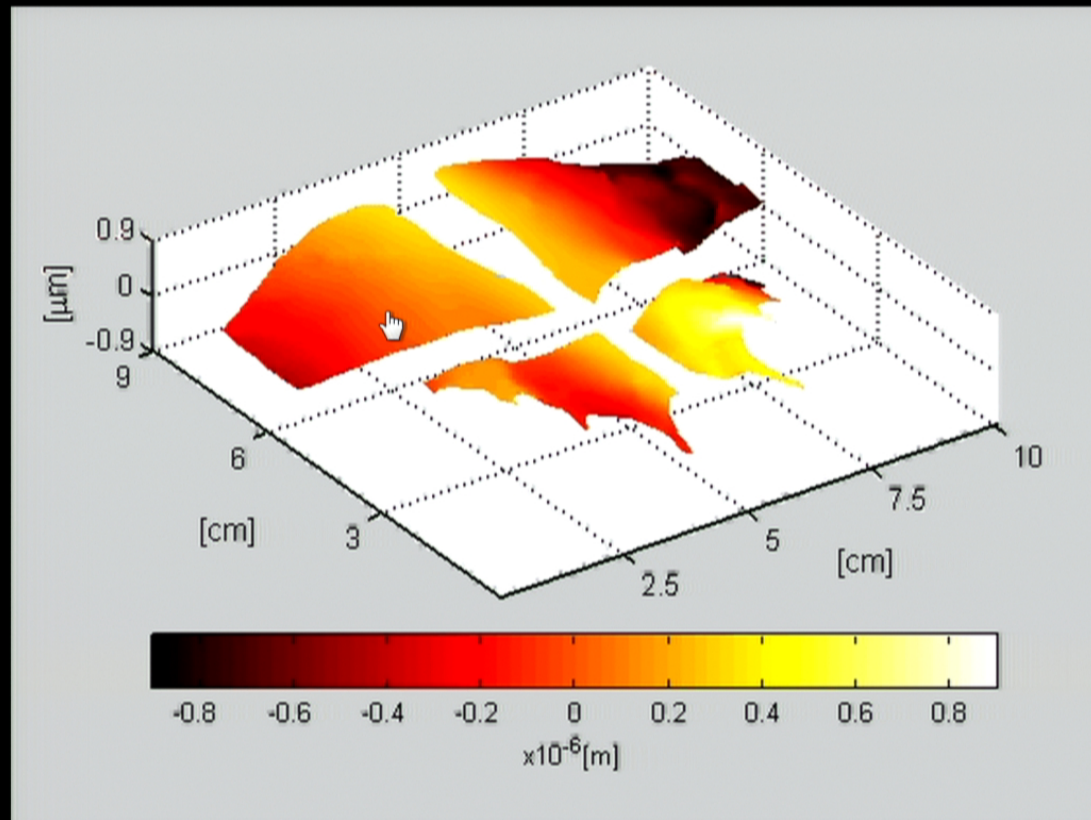
- in-vivo experimentation
- High speed DHI
- Laser Verdi (Coherent V6)
- Illumination density on the insecto:
19.6 mW/cm²
- NAC GX-1 camera
- Recordings at 4000 fps
- FOV: 90 x 100 mm
- 800 x 800 pixels
- 10 bits dynamic range



Unwrapped phase maps



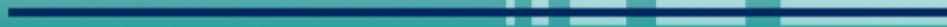
5. Resultados Experimentales

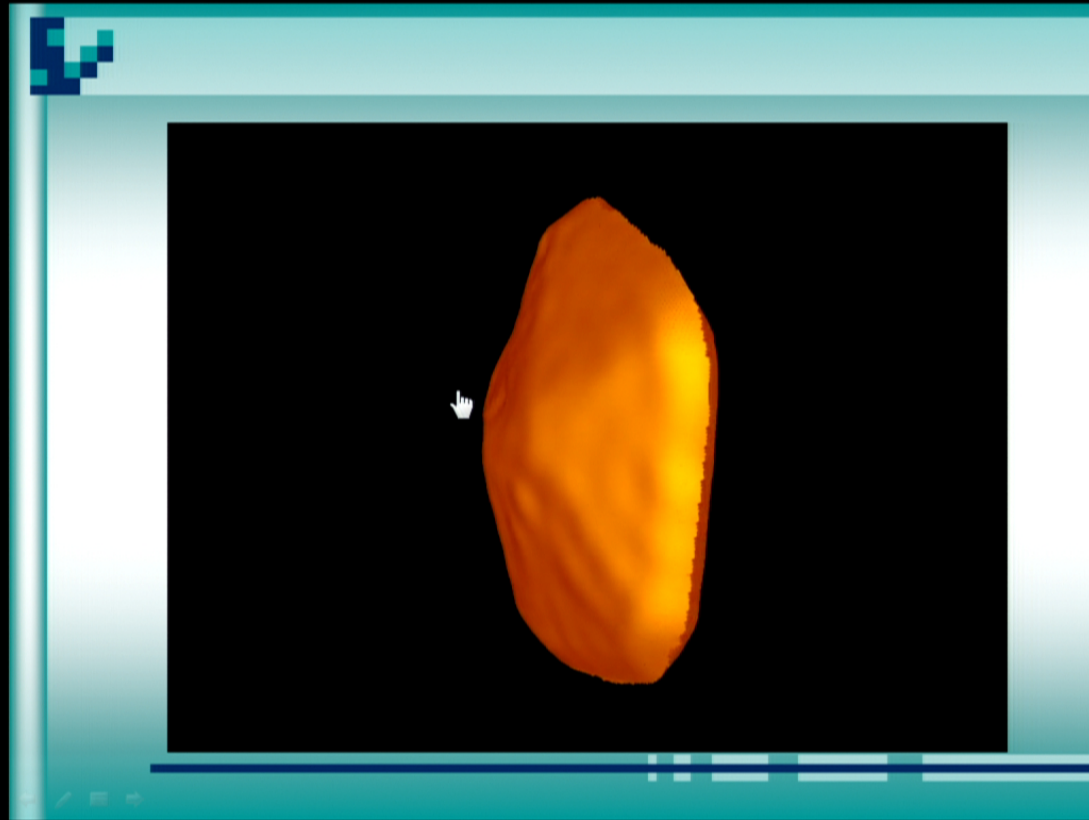


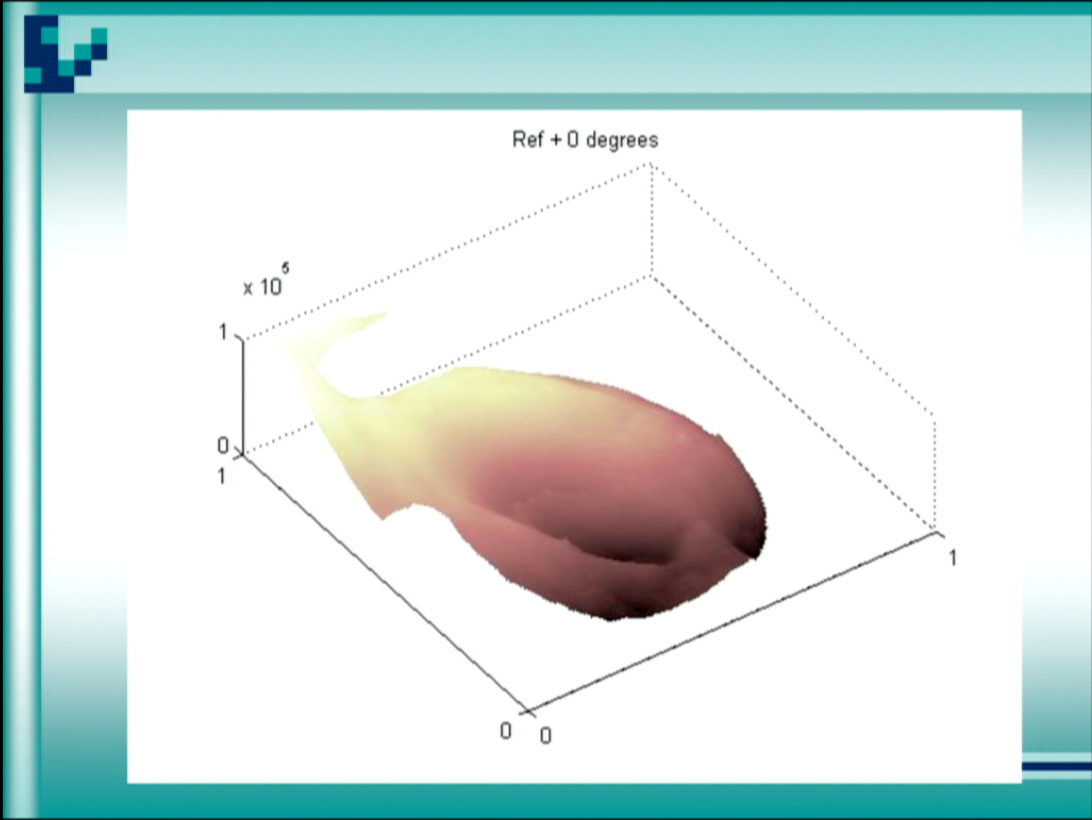


BACTERIA AND NANOPARTICLES

Determination of the surface morphology of gold-decahedra nanoparticles using an off-axis electron holography dual-lens imaging system, **accepted in Micron**









Research Team

- Dra. María del Socorro Hernández Montes
- Dr. Carlos Pérez López
- Dr. Manuel De la Torre Ibarra
- Dr. Jorge Mauricio Flores
- Jesus Cantu, Dr. Arturo Ponce and Prof. Miguel Jose Yacaman, UTSA

